Journal of Crystal Growth 70 (1984) 49–55
North-Holland, Amsterdam

HYDRODYNAMIC SIMULATION OF FORCED CONVECTION IN CZOCHRALSKI MELTS

Paulo H.O. RAPPL*, Luiz F. MATTEO FERRAZ, Hans J. SCHEEL*, Miriam R.X. BARROS and Dietrich SCHIEL

Instituto de Física e Química de São Carlos, Universidade de São Paulo, Caixa Postal 369, 13560 São Carlos SP, Brazil

Systematic hydrodynamic simulation experiments at room temperature were carried out in order to enhance the understanding of flow phenomena in Czochralski melts. An apparatus has been designed which allows the (three-dimensional) observation of hydrodynamic effects for various crucible shapes with adjustable rotation rates for crystal and crucible for iso- and counter-rotation. Also the effect of the accelerated crucible (and crystal) rotation technique (ACRT) on melt homogenization can be investigated. Flow visualization and measurement was done by ink injection, by light scattering of suspended particles and by the Schlieren technique, and laser doppler anemometry is foreseen. In this first report the results on forced convection in Czochralski melts and the occurrence ranges of specific flow regimes (like Cochran and Ekman flow, Couette and Taylor cells) and the transition from stable mixing to flow instability are discussed.

1. Introduction

In Czochralski melts the interplay of the various natural and forced convective regimes lead to temperature oscillations which are responsible for corresponding fluctuations of the growth rate and thus for striations in the crystals. Depending on the rotation rates of crystal and crucible, and depending on the sense of rotation (iso- or counter-rotation), the so-called Taylor–Proudman cells are formed, regions of liquid rotating quasi as a solid body with the crystal and the crucible. The occurrence of these cells in Czochralski melts, and their role in reducing the homogenization process of the liquid, were shown in the classical paper of Carruthers and Nassau [1] where hydrodynamic simulation experiments with injected ink were used to reveal the complex flow phenomena.

The main approaches to solve the striation problem have concentrated on the *reduction of convection*. Examples are the well-known experiments in microgravity and the use of convection-free cells or of baffles. More recently the application of magnetic fields in order to damp the convective oscillations, following the early suggestions of Utech and Flemings and of Hurle [2], has become popular to produce crystals of improved homogeneity.

An alternative approach to homogenization of Czochralski-grown crystals has been the application of *forced convection* by Scheel and Müller-Krumbhaar [3] using the Accelerated Crucible Rotation Technique [4,5]. Under specific ACRT conditions the formation of Taylor–Proudman cells can be prevented as it was shown in the two-dimensional numerical simulations of Mihelčić et al. [6].

Numerous hydrodynamic and numerical simulation experiments of Czochralski melts have been carried out; however, the computer simulations (e.g. Kobayashi and Arizumi [7], Langlois and Shir [8]) have been performed assuming rotational symmetry (two-dimensional simulations) and an idealized geometry. Nevertheless a sufficient knowledge of the fluid flow phenomena, allowing the improvement of homogeneity of Czochralski-grown crystals, is lacking. Specifically, the time-dependence of the three-dimensional flow under realistic geometrical and thermal conditions, taking into account the meniscus and non-flat crucible bottoms, needs to be studied. The present work was planned as a first step for such a study, where in addition to normal Czochralski growth, also the application and optimization of

* Present address: INPE, Avenida dos Astronautos, 12200 São José dos Campos SP, Brazil.

0022–0248/84/$03.00

ACRT would be investigated firstly by systematic hydrodynamic simulation experiments, secondly by three-dimensional numerical simulations to be carried out by Mihelčić et al. at KFA Jülich/FRG, thirdly by crystal growth experiments using the numerically optimized data, and fourthly by characterization of the crystals.

In this paper the experimental setup for the hydrodynamic simulation experiments and the visualization techniques will be described in the next section and followed by a description of the first results obtained for the case of forced convection, thereby neglecting initially the important role of buoyancy-driven and surface-tension-driven convection. An interesting result is the relatively sharp transition from quasi-laminar fluid mixing to instability in ACRT-mixed melts.

2. Hydrodynamic simulation apparatus

The setup consists of a Czochralski configuration with rotatable container and crystal, of an electronic part for adjustable rotation and acceleration rates, and of four interchangeable flow visualization and measurement systems. Fig. 1 shows the simulation apparatus with the ACRT electronics in the rack below, the motor-crucible-crystal-motor configuration, and the ink injection system.

2.1. Czochralski configuration

The rotatable crucible and the simulated crystal (INOX cylinder of 33.3 mm diameter) are mounted on two vertically aligned drill-machine tables; the vertical height adjustment is done using the cog-rail of the original drill-machine. The DC motors used for rotation are mounted on a double configuration of heavy steel plates and rubber pieces in order to minimize vibrations in a wide frequency range, and the rotation was transmitted to the axes by belts.

The silica glass crucible with rounded bottom (original from the silicon puller) or alternatively a glass crucible with flat bottom (internal diameter 100 mm) were mounted within a cubic Lucite container filled with a refractive-index-matched liquid (water–glycerine) in order to minimize the distortions of the cylindrical crucibles.

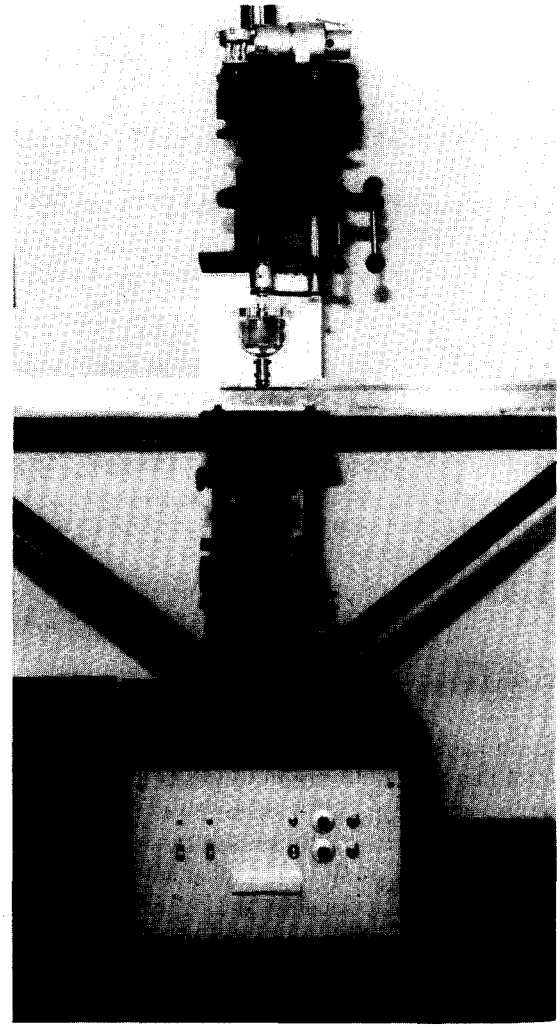

Fig. 1. Hydrodynamic simulation apparatus.

2.2 ACRT electronics

The ACRT method is being applied in numerous laboratories and industries where the periodic acceleration and deceleration of motors have been achieved by electronic or electromechanical means. However, for the convenience of other laboratories, we give in the following a brief description of the relatively simple electronic control system for dc motors used in the present investigation:

The digital part of the circuit consisting of a clock generator, an 8-bit up/down counter and an 8-bit

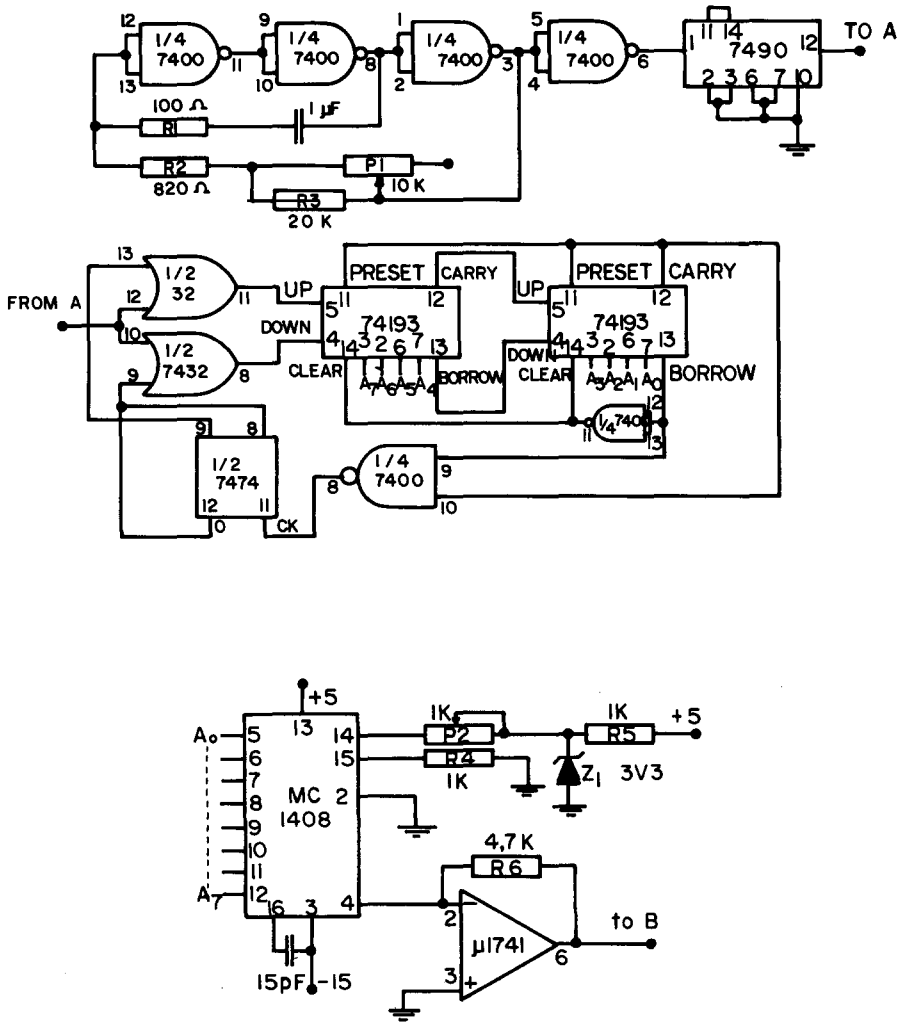

Fig. 2. Digital part of ACRT electronics with clock generator, up/down counter and A/D converter.

A/D converter is shown in fig. 2. The period of the generated pulses can be adjusted between 10 and 100 ms by the potentiometer P1. These pulses are counted by the up/down counter and converted to a triangular wave of a maximum amplitude of 10 V with periods adjustable between 12 and 114 s.

The analogue part of the circuit is shown in fig. 3. By the operational amplifier IC1, a 5 V signal (negative in relation to ground) is added to the wave signal and reduced by a factor 10 so that now a symmetric triangular wave varying between -500 and $+500$ mV is obtained. With the amplifier IC2 (gain setting by P5) a triangular wave is obtained of which the signal gain and/or frequency can be independently adjusted. This wave can now be injected into IC4 which through T1, T2, T3 to T6 will supply the voltage and current of the DC motor M1. The motor can also rotate at a constant rate, or oscillate within a given rotation range, through the level dislocation stage IC3 which moves the signal input between plus or minus V_{cc} with the potentiometer P8.

The possibility that transients due to the switching of the brushes of the motor rotor damage transistors T5 and T6 is prevented by an LC filter in the motor line.

A second motor can be synchronized with the first

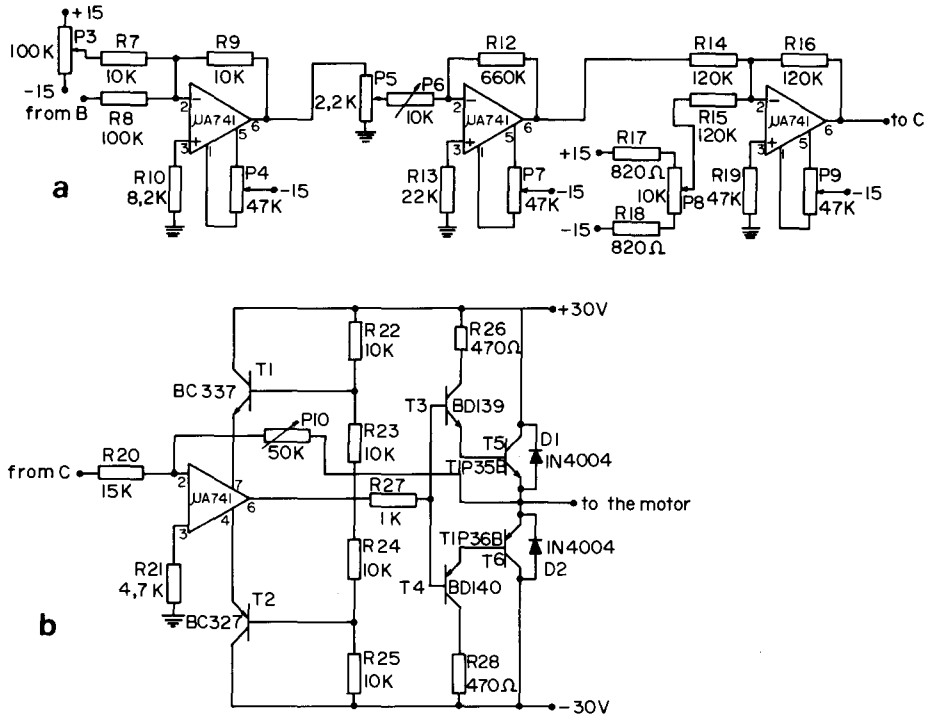

Fig. 3. Analogue circuit of ACRT electronics.

motor if the respective second analogue part is connected at point B. The synchronization can be iso- or counter-rotation by an inverter switch at one of the two motors.

2.3. *Flow visualization and measurement*

In order to achieve a most complete evaluation of the complex flow characteristics in the Czochralski melts, and specifically at the critical regions of the crystal–liquid interface, the free liquid surface and the crucible–liquid interface, the following four different flow visualization and measurement systems have been applied (one is being set up).

2.3.1. *Ink injection*

Through well-centered 0.5 mm capillaries of various lengths (passing through a central hole of the simulated crystal) a reproducible volume of ink could be injected into the simulated melt at various heights. A short injection time was applied in order to reduce the time of disturbance and in order to achieve quickly a high colour contrast, whereas Hide and Titman [9] used slow ink injection. The ink was distributed in the liquid and indicated the flow directions first from the center of the liquid and subsequently in the other parts of the crucible. Using two 500 W photolamps and white reflection screens, sufficient luminosity was achieved for taking video films with a 1 inch SABA camera and a Panasonic VHS NV 366 video-recorder.

Care was taken to use an ink liquid of equal density and viscosity which was achieved by dissolving the dye (methylene blue) in the simulation liquid. Nevertheless a significant disturbance of the flow was observed in the initial phase after ink injection, especially when relatively large ink volumes (> 1 ml) were injected with a high speed. It was discovered in the light scattering experiments that in certain critical cases ink injection induced flow patterns which were not genuine.

2.3.2. *Schlieren method*

The Schlieren method [10,11] allows to detect very small differences of refractive indices and thus to follow homogenization processes. Because lasers

cause undesirable speckle and other interference patterns, we used as light source a 625 W lamp (from an overhead projector) within a well-ventilated lamp holder. The lamp filament is projected by a lens (f = 5 cm) onto the entrance slit. Two mirrors of 10 cm diameter and f_1 = 125 cm, f_2 = 50 cm were used for projection in the Z-configuration [11].

The sensitivity of the system was tested by induced temperature variations of water for three light sources: the 1 mW He–Ne laser detected 0.5 °C, the 500 W Hg lamp 0.3 °C, and the overhead projection lamp 0.1 °C, the latter value corresponding to a refractive index change of 1×10^{-5}. With future larger mirrors and improved equipment a significant enhancement of sensitivity is expected.

The best Schlieren observation was possible with the cubic Lucite box and index-matched liquids inside and outside the crucible. A somewhat reduced sensitivity was noticed when instead of the liquid-filled box a second cylindrical container with liquid was used (as lens) to compensate the distortion of the observation container. Optimum resolution is observed in the direction perpendicular to the slit which therefore has to be adjusted according to the area of specific interest. The light intensity is just sufficient for filming with a 1 inch video-camera.

Although it is possible to observe the global flow patterns by the Schlieren technique (depth of focus greater than 10 cm) its specific strength lies in the observation of flows and fluctuations near the boundaries, for instance at the crystal–liquid interface in Czochralski growth, and of temperature variations.

2.3.3. Light scattering

One or two parallel beams from the 625 W overhead projector lamps were projected from the sides into the simulation chamber through slits of 6 mm width. By using suspended particles and observation from the front side the flow characteristics could be clearly followed in the illuminated vertical or horizontal plane of the liquid by the motion of the light-scattering particles. Instead of the aluminium powder described in Greenspan's book [12] we used water-saturated screened pinewood particles in a density-matched aqueous solution of KI.

Most fluid phenomena can be observed by light scattering. However its specific strength lies in the detection of instabilities and vortices. By photographing with defined exposure times and by measuring the streak lengths in the photographs the distribution of velocity components parallel to the illumination plane can be evaluated.

2.3.4. Laser anemometry

In Laser Doppler Anemometry (LDA) two laser beams, obtained by beam-splitting of a single laser, intersect in a point of moving fluid with suspended scattering particles. The scattered light shows a Doppler frequency shift which is proportional to the particle velocity and which can be determined by mixing with a reference beam on the surface of a photodetector. The STI instrument [13] is being mounted onto a mechanical height and distance displacement table which allows to adjust the measurement point within the simulation crucible.

The advantages of LDA are a relatively high precision of the velocity measurements (for steady flow) and the relatively high local resolution. The disadvantage is the point-wise detection so that for the velocity distribution in a complex flow system the light-scattering photography is preferred.

3. Experiments

In initial experiments the fluid phenomena were studied by the distribution of ink in the simulation liquid (water) after the injection of 0.3 ml ink solution. For short ACRT periods (τ = 12 s), there was no difference found between various crucible shapes with round and flat bottoms. As always ACRT of crucible and/or crystal was used with velocity changes of either 0–20 or 0–60 rpm, no Taylor–Proudman cells could be observed, neither for counter- nor for iso-rotation. With low crucible ACRT values little mixing was found, whereas at vigorous ACRT action very efficient mixing was observed which, however, would probably cause problems in crystal growth. After these preliminary results more systematic experiments were done with the light-scattering technique.

In these experiments, using pinewood particles suspended in an aqueous solution of KI of density 1.60 g/cm^3 and a viscosity of 1 cP (ν = 0.64 cSt), only a crucible with a flat bottom was applied.

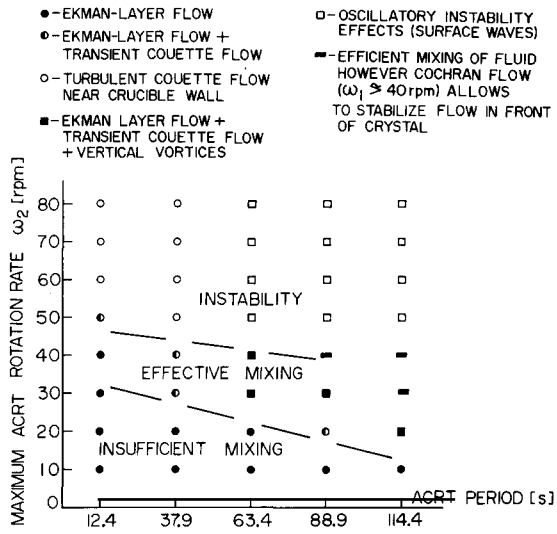

Fig. 4. Regions of insufficient and efficient mixing and of instability in systematic ACRT simulation experiments using aqueous KI solution of $\nu = 0.64$ cSt.

Although the ACRT parameters (period, maximum rotation rate) were varied in a wide range (see fig. 4), Taylor–Proudman cells could not be observed for a stationary crystal. Even with a constantly rotating crystal (and ACRT of crucible) the Taylor–Proudman cells are not pronounced if existing at all, and the crystal causes Cochran flow of an intensity depending on the rotation rate of the crystal ω_1.

In systematic light-scattering experiments the maximum ACRT crucible rotation rates ω_2 in the range 10 to 80 rpm, and ACRT periods in the range 12.4 to 114.4 s were applied. Regions of specific or combined flow regimes can clearly be distinguished as indicated in fig. 4. A region of effective mixing (consisting of Ekman-layer flow, transient Couette flow and vertical vortices) can be defined for ACRT parameter 40 rpm/12.4 s to 20–30 rpm/114.4 s. At lower ω_2 the homogenization of the liquid is not sufficient and is accomplished only by weak Ekman-layer flow. At high ω_2 values obviously the mixing is very efficient; however, the resulting instabilities and especially the surface waves probably would cause problems for crystal growth.

These results should be taken with care due to the high sensitivity of stability limits and flow regimes to vibrations and to the precision and alignment of the system.

4. Discussion

Hydrodynamic simulations allow a three-dimensional evaluation of Czochralski flow with relatively simple means. The initial experience with various flow visualization methods has demonstrated their specific strengths and also that a critical comparison of the results obtained with the different methods helps to prevent misinterpretations. In view of the hydrodynamic complexity of the problem, especially when ACRT is applied to Czochralski growth with six different flow regimes, it is necessary to make a systematic step-by-step approach. Thus we have limited the first studies to an isothermal system with forced convection only. It was shown that the undesirable Taylor–Proudman cells can be prevented by application of ACRT. However, when at a later stage a realistic temperature distribution (and thus buoyancy-driven and Marangoni convection) has to be taken into account, the preservation of an acceptable flat or slightly convex crystal interface will drastically restrict the tolerable parameter range of ACRT. Another problem is the transfer of room-temperature simulations with liquids of high Prandtl numbers to the high-temperature liquids with very small Prandtl numbers like semiconductors and metals. This transfer has to be done numerically. So one can conclude that in principle it is possible to homogenize Czochralski melts by ACRT, and a stable flow regime in front of the crystal can be achieved by proper adjustment of the crystal-rotation rate, and thus of the Cochran flow.

Acknowledgements

With pleasure we acknowledge the technical assistence of Luiz Barsi and the fabrication of mirrors and lenses in the optical shop of Professor Jarbas C. Castro Neto, and we appreciate the initial support from Professor Nilton F. de Souza. Valuable discussions were held with Dr. M. Mihelcić, Professor H. Müller-Krumbhaar and Professor H. Wenzl. The work was supported by the research foundation of the Banco do Brasil – FIPEC, by CAPES and CNPq.

References

[1] J.R. Carruthers and K. Nassau, J. Appl. Phys. 39 (1968) 5205.
[2] H.P. Utech and M.C. Flemings, J. Appl. Phys. 37 (1966) 2021;
D.T.J. Hurle, in: Crystal Growth, Ed. H.S. Peiser (Pergamon, Oxford, 1967) 659.
[3] H.J. Scheel and H. Müller-Krumbhaar, J. Crystal Growth 49 (1980) 291.
[4] H.J. Scheel and E.O. Schulz-Dubois, J. Crystal Growth 8 (1971) 304.
[5] H.J.Scheel, J. Crystal Growth 13/14 (1972) 560.
[6] M. Mihelčić, C. Schroeck-Pauli, K. Wingerath, H. Wenzl, W. Uelhoff and A. Van der Hart, J. Crystal Growth 53 (1981) 337.
[7] N. Kobayashi and T. Arizumi, J. Crystal Growth 30 (1975) 177.
[8] W.E. Langlois and C.C.Shir, Computer Methods Appl. Mech. Engng. 12 (1977) 145.
[9] R. Hide and C.W. Titman, J. Fluid Mech. 29 (1967) 39.
[10] E.B. Brown, Modern Optics (Krieger, Huntington, NY, 1974) p. 466.
[11] T.P. Davies, Opt. Laser Technol. 13 (1981) 37.
[12] H.P. Greenspan, The Theory of Rotating Liquids (Cambridge University Press, 1969).
[13] TSI Thermo-Systems Inc., St. Paul, Minnesota (35 mW He–Ne laser Spectra-Physics Model 124B, Optical Units TSI 910, Photomotoplier TSI 9162, Input Conditioner TSI 1984, Timer TSI 1985, Readout TSI 1992), kindly provided by Professor Geraldo Lombardi, EESC/USP.